Full range of proximity effect probed with Superconductor/Graphene/Superconductor junctions

Chuan Li, S. Guéron, A. Chepelianskii, and H. Bouchiat

Laboratoire de Physique des solides, Univ. Paris Sud

The high tunability of the density of states of graphene [1] makes it an ideal probe of quantum transport in different regimes. In particular, the supercurrent that can flow through a non-superconducting (N) material connected to two superconducting electrodes, crucially depends on the lenght of the N relative to the superconducting coherence length. Using graphene as the N material we have investigated the full range of the superconducting proximity effect, from short to long diffusive junctions. By combining several S/graphene/S samples with different contacts and lengths, and measuring their gate-dependent critical currents (I_c) and normal state resistance R_N, we compare the product $eR_N I_c$ to the relevant energies, the Thouless energy in long junctions and the superconducting gap of the contacts in short junctions, over three orders of magnitude of Thouless energy. The experimental variations strikingly follow a universal law, close to the predictions of the proximity effect both in the long and short junction regime, as well as in the crossover region, thereby revealing the interplay of the different energy scales. Differences in the numerical coefficients reveal the crucial role played by the interfacial barrier between graphene and the superconducting electrodes, which reduces the supercurrent in both short and long junctions. Surprisingly the reduction of supercurrent is independent of the gate voltage and of the nature of the electrodes. A reduced induced gap and Thouless energy are extracted, revealing the role played by the dwell time in the barrier in the short junction, and an effective increased diffusion time in the long junction. We compare our results to the theoretical predictions of Usadel equations and numerical simulations which better reproduce experiments with imperfect NS interfaces.

PACS numbers:

The superconducting proximity effect describes the phenomena that occur when a superconductor (S) is placed in contact with a non-superconducting conductor ("normal" conductor, N), and superconducting properties are induced in the N due to the propagation of correlated Andreev pairs from the superconductor to the N [2]. Several experiments have revealed the striking effects of induced superconductivity: density of states measurements with tunnel probes have shown how the pair correlations develop as a function of distance to the NS interface [3]; how a minigap is induced in the N when it is connected to two S, and how this minigap is modulated by a magnetic flux that induces a phase difference between the two S electrodes [4]. In fact, not only the minigap but the entire energy spectrum of the Andreev eigenstates is phase-dependent, leading to a dissipationless supercurrent that can flow through the normal conductor. The phase dependence of the supercurrent has been probed both at high and low frequency [5]. It is remarkable that all the aforementioned experiments could be described by the theory of the proximity effect, irrespective of the superconducting and normal metals used, their length, aspect ratios, and diffusion constants. The universality of the proximity effects stems from the diffusive motion of carriers, that links the distance pair correlations can travel to a characteristic diffusion time, and hence an energy. A striking example of this universality is given by the maximum supercurrent that can flow through a diffusive SNS junction, called the critical current. The theory of the proximity effect predicts that the critical current is proportional to the smallest correlation energy scale of the problem: the gap energy of the superconducting electrodes if the N is shorter than the superconducting coherence length, or the Thouless energy, proportional to the inverse diffusion time through the N, in the case of long junctions. The full length dependence of the critical current, from short to long diffusive junctions, was calculated in Dubos [9], and provides a stringent test of the universality of the proximity effect. This prediction has to our knowledge not yet been tested.

An instance where the universality of the proximity effect could break down is when the interfaces between the N and the S are non ideal. Fermi velocity differences between the N and S materials, disorder, Shottky, or insulating barriers at the interface, often cause an interface resistance, that limits the number of induced Andreev pairs, and thus the critical current. The way the critical current is modified in both the short and long limits has been addressed theoretically [8, 10, 31], but is difficult to test experimentally, since metallic SNS junctions are not tunable. Each junction is unique, with a sample-dependent interface resistance that is often difficult to disentangle from the intrinsic resistance of the normal metal.

In this Letter, we test the universality of the proximity effect in diffusive SNS junctions, from the short- to long-junction regime, over an unprecedented three order of magnitude range of the Thouless energy over gap ratio. This is made possible by using graphene as the normal conductor in S/graphene/S (SGS) Josephson junctions.

Indeed, graphene's carrier density can be controlled by a gate voltage, leading to the possible continuous spanning, in a single sample of given length L and aspect ratio, of both the Fermi wave-vector and the diffusion constant D, and thus the Thouless energy $E_{Th} = \hbar D/L^2$[11, 14].

We track the critical current I_c of seven diffusive graphene samples, using three different superconducting materials, over a wide range of gate voltage. We find that the product $R_N I_c$ of the critical current by the normal state resistance is proportional to an effective Thouless energy that is a fraction of the Thouless energy, for all long junctions investigated. In the short junction limit, we find that the $R_N I_c$ product is independent of the Thouless energy, and that it is smaller than the electrodes superconducting gap Δ. We find that data of all samples collapse on a single curve, that we compare to the theoretical prediction of the Usadel equations. In addition, we perform numerical simulations of the proximity effect in the experimentally relevant situation of an interface with a partial transmission. The simulations reproduce qualitatively the behavior suggested by the experiments, underscoring the role played by multiple inner reflections of Andreev pairs that increase the dwell time in the N conductor.

The critical current of short diffusive SNS junctions ($\Delta/E_{Th} \to 0$) is predicted to obey ([6, 7])

$$eR_N I_c \simeq 1.326\pi\Delta/2 \simeq 2.07\Delta. \tag{1}$$

Whereas the full superconducting gap Δ is induced in N in short junctions, in long-junctions ($\Delta/E_{Th} \to \infty$) a much smaller , or "mini" gap Δ_g is induced in the N. Δ_g is proportional to the Thouless energy: $\Delta_g \simeq 3.1 E_{Th}$ [28]. The product $eR_N I_c$ at zero temperature is also proportional to E_{Th} [9]:

$$eR_N I_c(T=0) = 10.82 E_{Th} = 3.2\Delta_g. \tag{2}$$

Expressions (1) and (2) show that it is the smallest of the two energies, Δ and E_{Th}, that limits the critical current in diffusive SNS junctions. The crossover between the short and long junction regimes was also investigated using Usadel equations [9], and it is found that throughout the full proximity effect range, only the diffusive constant, sample length and superconducting gap determine the critical current, regardless of sample geometry. This universality is unique to the diffusive regime: in ballistic SNS junctions, the critical current is expected to depend on the detailed geometry of the samples [29]. Expression (2) was found to reproduce quite well experiments on long metallic SNS junctions [30] with a good transmission at the SN interface. It was however shown [8, 10, 31] that (1) and (2) are modified by interfacial barriers. The barriers are characterized by an energy scale $\gamma = \hbar/\tau_\gamma$, with τ_γ the typical time associated with the barrier transmission. The barrier can be of various types: tunnel, Schottky or due to disorder at the NS interface, a higher barrier corresponding to a longer dwell time and shorter γ. When γ

is smaller than the superconducting gap, $eR_N I_c$ for short junctions is limited by γ, and independent of Δ [10]. The situation is more complex in long junctions with an interfacial barrier such that $\gamma > E_{Th}$, and was less investigated theoretically. The interfacial barrier is often modeled by a simple resistance $R_c \sim h/e^2 M\tau$ due to M conduction channels of identical transmission $\tau < 1$, and characterized by the ratio $r = R_c/(R_N - 2R_c)$, where R_N is the total normal state resistance, i.e. that of the conductor and barrier resistances in series. In the high r limit, it was found that in short junctions the induced gap Δ^* (defined as $eR_N I_c/2.07$) is reduced according to $\Delta^* = \Delta/r$. In long junctions (2) is also predicted to be modified with a reduction of the minigap and critical current that essentially depends on r and practically not on τ [31].

In the following we present our experimental results on S/graphene/S junctions differing by their superconducting electrodes, length and mobility. Varying the doping changes r substantially, revealing a striking universal behavior, and offering a stringent test of theoretical predictions.

All the samples reported in this paper were prepared by mechanical exfoliation onto oxidized substrates of highly doped Si. Sample parameters are given in table I. The Ti/Al contacts are e-beam evaporated and the Pd/Nb and Pd/ReW contacts are dc-sputtered. The sample length L varies from 300 nm to $1.2\mu m$ and the ratio ξ_s/L, where $\xi_s = \sqrt{\hbar D/\Delta}$ is the superconducting coherence length, varies from 10 to 0.3, so that the full range from short to long junction is accessed for the first time.

The gate-voltage-dependence of the normal state resistance $R_N = 2R_c + R_G$ yields both the contact resistance $2R_c$ and the intrinsic graphene resistance R_G. Within a good approximation R_G is found to vary like $1/|V_g - V_D|$ [1] at high gate voltage V_g relative to the Dirac point V_D. R_c is found to be independent of V_g, and is obtained by the linear extrapolation of $R_N = f(x = 1/|V_g - V_D|)$ close to $x = 0$. We can then determine the conductivity $\sigma = \rho^{-1} = (R_G W/L)^{-1} = (2e^2/h)(k_F l_e)$ and deduce the mean free path l_e, the diffusion coefficient $D = 1/2v_F l_e$, and the Thouless energy. The Fermi wave-vector k_F is deduced from a simple capacitance model, valid away from the Dirac point [27]. The elastic mean free path l_e varies with V_g from 50 nm to 160 nm. Our samples are thus always in the diffusive regime. The contact resistance R_c, between tens and hundreds of Ohms (see table), corresponds to a rather uniform product of contact resistance by sample width, of the order of 250 $\Omega \pm 50$ μm. R_c is thus negligible at low doping, but can be of the order of, or even larger than, the intrinsic resistance of graphene at high doping. This is an ideal parameter range to test the dependence of the proximity effect with r. Using the expression for the conduction channels $M = k_F W/\pi$, that yields roughly 80 channels for a micron-wide sample at $V_g - V_D = \pm 30$ V, one can
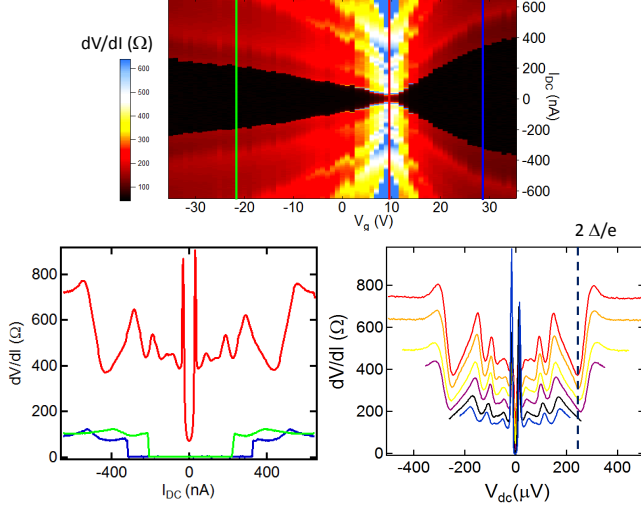
FIG. 1: Top: Color-coded plot of dV/dI as a function of gate voltage and dc current. Black corresponds to zero resistance. Bottom left: Differential resistance $dV/dI(I_{DC})$ at three different gate voltages, including at $V_G=0$V, close to the Dirac point (red curve). The resistance jumps from zero to the normal state resistance at the critical current I_c. The peaks in the differential correspond to Multiple Andreev reflections as clearly seen on the right plot where the same data is shown as a function of the dc voltage drop through the sample.

then deduce the average transmission τ of the contacts via $R_c = (h/4e^2)M^{-1}(1/2 + (1 - \tau)/\tau)$ [35], and we find $\tau = 0.25 \pm 0.1$.

The differential resistance of the samples was measured at 100 mK via filtered lines, using a standard lock-in technique. Fig. 1 displays the colour-coded differential resistance as a function of the bias current and gate voltage, showing a gate-dependent critical current of the SGS junction Al1. The critical current is strongest at high doping, and depressed at gate voltages close to the Dirac point. Peaks in the differential resistance at $V_n = 2\Delta/ne$ are manifestations of the multiple Andreev reflections (MAR), typical of SNS junctions [33] and enable the determination of Δ.

All samples show qualitatively similar behaviors, with quantitative differences: in the long junction samples (Nb, ReW), the critical current is not just depressed, but is actually destroyed near the Dirac point. We attribute this striking suppression to the charge puddles in the sample near half filling, and the specular Andreev reflections across their boundaries, that randomize the phase of Andreev pairs [24]. In the following we focus on data sufficiently far from the Dirac point (Table I) so that the critical current is higher than 100 nA. This ensures that thermal fluctuations have a negligeable influence, since the corresponding Josephson energy $E_J = \Phi_0 I_c/2\pi$ is above 3 K, more than ten times the sample temperature[34]. We show in the following that all samples exhibit a universal behavior.
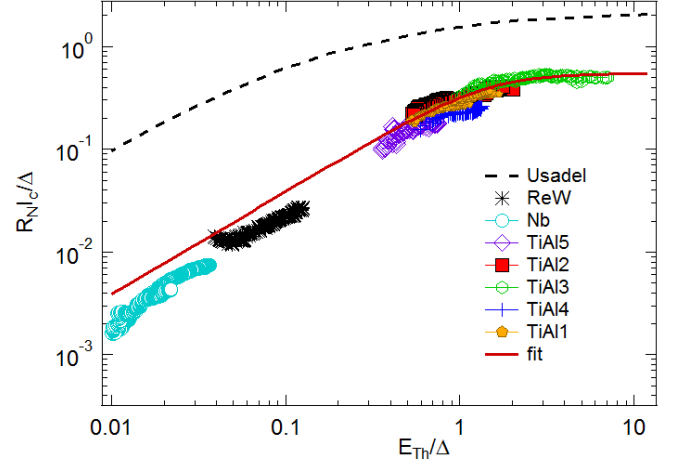

FIG. 2: Variations of $R_N I_c/\Delta$ with $x = E_{Th}/\Delta$ for seven diffusive SGS junctions, of different lengths and with different superconducting electrodes. The superconductor used as a contact is indicated in the legend. For each sample, a continuous range of Thouless energy is accessed by varying the gate voltage. Three orders of magnitude of Thouless energy over Delta are accessed. All data practically collapse on a single curve $F(x)$ (red continuous line), see expression (3), whose shape describes both the short and long junction limits, as well as the crossover between the two regimes. This shape is similar to the theoretical curve for a perfect interface, computed from the Usadel equations by Dubos et al.[9] (dashed black curve).

To follow and compare the critical current of all samples, we plot the experimentally determined $eR_N I_c/\Delta$ as a function of $x = E_{Th}/\Delta$, (Fig. 2), along with the numerical solution $F_U(x)$ of the Usadel equations for perfect interfaces [9]. We find that all experimental data nearly collapses on a single curve, $eR_N I_c/\Delta = F(x)$, with two asymptotic behaviors that clearly correspond to the long and short junction limits. This universal behavior of all the graphene-based SNS junctions we have investigated is the central result of our paper. In the short junction limit, $\lim_{x\to\infty} F(x) = a$ with $a = 0.55$, and in the long junction limit $\lim_{x\to 0} F(x) = bx$ with $b \simeq 0.39$. This behavior is qualitatively similar to the result of Usadel equations, although the Usadel equation coefficients are different: $a_U \simeq 2.07$ and $b_U = 10.82$ [9]. This comparison with Usadel equations leads us to define effective energies $\Delta^* = (a/a_U)\Delta \simeq 0.3\Delta$ and $E_{Th}^* = (\Delta/\Delta*)(b/b_U)E_{Th} \simeq 0.14E_{Th}$ such that $eR_N I_c/\Delta^* \to a_U$ in the short junction limit and $eR_N I_c/\Delta^* \to b_U E_{Th}^*/\Delta$ in the long junction limit. The full dependence, including the crossover between short and long junctions, can be fitted by a generic expression:

$$\frac{eR_N I_c}{\Delta} = F(x) = \frac{abx}{(a^n + b^n x^n)^{1/n}}. \qquad (3)$$

TABLE I: Characteristic parameters of the investigated samples.
The large contact resistances measured for the Al4 and Al5 samples are not intrinsic to the sample but due to silver paste connection problems

	Short/intermediate junction										long junction			
	Ti/Al(6nm/70nm)										Pd/Nb 8/70 nm		Pd/ReW 8/70 nm	
Sample	Al1		Al2		Al3		Al4		Al5		Nb		ReW	
L (nm)	500		400		350		450		500		1200		700	
W (μm)	3.4		4		4		4		4		12		5	
$\overline{l_e}$ (nm)	120		140		150		120		170		60		70	
$\overline{\xi_s}$ (nm)	400		500		430		420		520		120		120	
R_c (Ω)	158	136	105	110	172	170	N.A.	860	862	853	40	60	98	120
V_g (V) range	-35 -2.5	$+16.5$ $+35$	-35 -10	$+15$ $+25$	-30 -5	$+5$ $+30$	N.A.	-10 $+5$	-30 -20	$+12$ $+30$	-30 -3	$+10$ $+20$	-25 $+5$	$+15$ $+25$

Fig. 2 shows that the Usadel results are very well fitted by $n \simeq 1$, and the experiments, with a sharper crossover, by $n \simeq 2$. Fig. 2 also shows that an imperfect interface does not change the main features of the proximity effect: in short junctions $R_N I_c$ is independent of E_{Th}, and in long junctions $R_N I_c$ varies linearly with E_{Th}. According to refs.[8, 10], the reduced effective gap Δ^* should just be γ, the inverse characteristic transmission time through the NS barrier in the limit where $\Delta \gg \gamma \gg E_{Th}$. It is interesting that the Δ^* we find is sample independent, for the three samples with Ti/Al contacts for which the crossover between long and short junction is accessed. One would have liked to test samples with different superconducting gaps in this short junction regime to determine whether $\Delta^* = \gamma$ is independent of Δ. This was not possible for the Pd/ReW and Pd/Nb contacts, whose very small superconducting coherence length would require sub 30-nm-size junctions to reach the short junction limit.

The physical meaning of the crossover between short and long junctions in the presence of barriers can be heuristically understood writing that $e R_N I_C = \hbar/\tau_{dw}$, where τ_{dw} stands for the typical traversal time of the SNS junction, which is the sum of τ_γ, the time spent in the barriers, and τ_D, the diffusion time through the normal junction, yielding $e R_N I_c = \gamma E_{Th}/(E_{Th} + \gamma)$. This expression reproduces quite well the solution of the Usadel equations [9], with γ instead of Δ, and corresponds to eq. (3) with n=1. Its dependence is similar to the experimental curve, although the theoretical crossover is smoother than the experimental curve, that is better described by n=2.

We now turn to the long junction regime, in which the critical current varies linearly with E_{Th}, but is smaller than the theoretical prediction for perfect interface by a factor $b_U/b \simeq 33 = 3E_{Th}/E_{Th}^*$ [9]. In [32] we show that this reduced Thouless energy E_{Th}^* also determines the temperature dependence of I_c.

Modifications of $I_c(0)$ and $I_c(T)$ due to imperfect interfaces were investigated by Hammer et al. [31] us-

ing the Usadel equations formalism. They predict that the renormalised critical current and its variations with temperature depend not only on E_{Th}/Δ but also on $r = R_c/(R_N - R_c)$, with a drastic reduction of $R_N I_c$ at high r. Since r varies in graphene by a factor 50 ($r \simeq 0.1$ close to $V_g = V_D$, and $r \simeq 5$ around $V_g \simeq 30$ V), one would expect E_{Th}^*/E_{Th} to vary with doping, in strong contrast to the universal behavior suggested from our data. The same calculation also predicts a critical current that is only barely reduced so long as the interface resistance is small relative to the normal conductor's resistance ($r \ll 1$). For $r = R_c/R_N \simeq 0.1$ for instance, as in our experiments at low doping, the prediction would be $b/b_U \simeq 1$ (using our notations). This is in stark contrast with our experimental finding of $b/b_U \simeq 0.03$. Such a high reduction due to a relatively small interface resistance was already reported by Dubos et al.[9] in a metal SNS junction.

A possible interpretation of a strongly reduced effective Thouless energy ($E_{Th}^* \ll E_{Th}$) could be the repeated inner reflections of Andreev pairs at the interfacial barriers, leading to an increased typical time spent in the SNS junction from τ_D to $N\tau_D$, where N is the number of reflections at the NS interfaces.

We now present numerical simulations, in which we do find a strongly (ten-fold) reduced critical current, even for $r \ll 1$, i.e. a graphene sheet whose intrinsic resistance is much higher than the interface resistance. We implement the Bogoliubov-de Gennes Hamiltonian that describes the electron- and hole-like wavefunction components of a hybrid NS ring in a tight-binding 2D Anderson model [37]. The graphene sheet is a hexagonal lattice oriented along the armchair direction with $N_x \times N_y$ sites, and is connected to two superconducting electrodes ($N^S = N_x^S \times N_y$ sites on a square lattice), see inset of Fig. 3. Disorder is described by random on-site energies of variance W^2. The hopping matrix element is restricted to nearest neighbors $t_{ij} = t$. The SN interface barrier is taken into account via a reduced hopping amplitude between the N and S sites: $|t_{SN}/t|^2 = \tau$, with
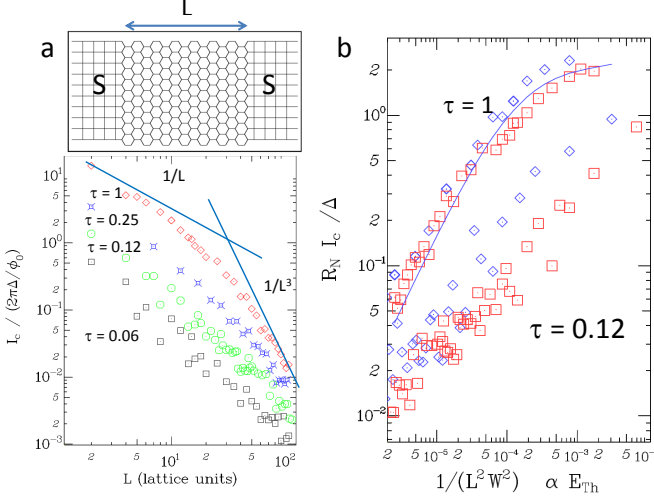
FIG. 3: a- Length dependence of the Josephson current calculated for a diffusive graphene ribbon between superconducting electrodes for different values of τ. The number of transverse channels is $N_y = 60$, the disorder is $W = 6$. b- The product $R_N I_c$ is shown as a function of $1/W^2 N_x^2$ (that is proportional to the Thouless energy), for 2 different values of disorder (W=6, red symbols, and W=9, blue symbols.)

$0 < \tau < 1$, [38] The Josephson current $I_J(\varphi) = \partial E_J/\partial\varphi$ is the derivative of the Josephson energy E_J, the sum of the occupied, phase-dependent energy levels. The critical current I_c is the maximum of $I_J(\varphi)$. Fig. 3 displays the length dependence of I_c of a graphene ribbon with $N_y = 60$ and the dependence of $R_N I_c$ with Thouless energy. When $\tau = 1$ (perfectly transmitting interfaces), we find that I_c varies as $1/L$ in short junctions, i.e. for L smaller than the superconducting coherence length (of the order of 10 lattice spacings), in accordance with Eq. (1), $eR_N I_c \simeq 2.07\Delta$. For long junctions, a faster $1/L^3$ decay is observed, in accordance with Eq. (2), $eR_N I_c \simeq 10.8 E_{Th}$. R_c and R_N are estimated via $R_c = (1 - \tau)/N_y\tau + 1/N_y$ and $R_N = 2R_c + L/N_y l_e$. As expected, the simulation displays an approximately linear relation between $R_N I_c$ and E_{Th} in the long junction regime. More crucially, the simulations also show a striking reduction in the critical current of long junctions for an interface transmission τ of 0.12, even when r is smaller than 0.1. We also find this effect for a square lattice instead of a hexagonal lattice, demonstrating that it is not specific to graphene. This strong reduction of supercurrent by a relatively small resistance barrier, that we find in the experiment and in the simulations, is a central result of our paper. Such a reduction of the supercurrent is to our knowledge not predicted in [31].

In conclusion, we have tested the Thouless energy dependence of the critical current of diffusive SNS junctions over three orders of magnitude, thanks to the tunability of graphene used as the diffusive normal conductor. Our analysis of the critical current in different graphene-based

Josephson junctions in the diffusive regime shows a remarkable universal behavior, with a crossover between long and short junctions regimes. The full dependence of $R_N I_c$ Vs E_{Th}/Δ can be described by the result of the Usadel theory with perfect interfaces, provided a sample-independent rescaling of the superconducting gap and Thouless energy down to lower energies is performed. We understand this reduction as due to the barriers at the NS interface, whose transmission is estimated to be of the order of 0.25. We find that the predictions of Usadel equations in the long junction limit with opaque interfaces do not agree with the universal behavior we observe. A better agreement is obtained with numerical computation of the Andreev spectrum using a tight binding model of graphene. These results call for a better theoretical understanding of the influence of barriers at the N/S interface on the transmission of Andreev pairs through long SNS junctions.

[1] A. H. Castro Neto, F. Guinea, N. M. Peres, K. S. Novoselov, and A. K. Geim, *The electronic properties of graphene*, Rev. Mod. Phys. **81**, 109 (2009).

[2] P.G. de Gennes,*Boundary Effects in Superconductors*, Rev. Mod.Phys. **36**,225 (1964). Kulik, I.,*Macroscopic quantization and proximity effect in S-N-S junctions*, Sov. Phys. JETP **30**, 944 (1970).

[3] S. Guéron, H. Pothier, Norman O. Birge, D. Esteve, M.H. Devoret,*Superconducting proximity effect probed on a mesoscopic length scale*, Phys. Rev. Lett. **77**, 3025 (1996).

[4] H. le Sueur et al.,*Phase Controlled Superconducting Proximity Effect Probed by Tunneling Spectroscopy*, Phys. Rev. Lett. **100**, 197002 (2008).

[5] M. Fuechsle et al.,*Effect of Microwaves on the Current-Phase Relation of SuperconductorNormal-MetalSuperconductor Josephson Junctions* Phys. Rev. Lett. **102**, 127001 (2009).
B. Dassonneville, M.Ferrier, S. Guéron, and H. Bouchiat,*Dissipation and Supercurrent Fluctuations in a Diffusive Normal-MetalSuperconductor Ring*, Phys. Rev. Lett. **110** 217001 (2013).

[6] I. O. Kulik and A. N. Omel'yanchuk,*Contribution to the microscopic theory of the Josephson effect in superconducting bridges*, Zh. Eksp. Teor. Fiz. Pis. Red. 21, 216 [JETP Lett. 21, 96 (1975)].

[7] Likharev, K. K.,*Superconducting weak links*, Rev. Mod. Phys. 51, 101 (1979).

[8] A. A. Golubov, M. Yu. Kupriyanov and E. Illichev,*The current-phase relation in Josephson junctions*, Rev. Mod. Phys. 76, 418 (2004).

[9] P. Dubos, H. Courtois, B. Pannetier, F. K. Wilhelm, A. D. Zaikin, and G. Schön,*Josephson critical current in a long mesoscopic SNS junction*; Phys. Rev. B **63**, 064502 (2001); P. Dubos, H. Courtois, O. Buisson, and B. Pan-

netier,*Coherent Low-Energy Charge Transport in a Diffusive S-N-S Junction*, Phys. Rev. Lett. **87**, 206801 (2001). P. Dubos PhD Thesis (2001).

[10] Brinkman, A., and A. A. Golubov,*Coherence effects in double-barrier Josephson junctions*, Phys. Rev. B 61, 11297 (2000).

[11] The length dependence of the critical current was investigated in semiconducting nanowires in [12], with mainly short junctions, and metallic wires in [13], in the limit $r \gg 1$.

[12] S. Abay, D. Persson, H. Nilsson, F. Wu, HQ Xu, M. Fogelstrom, V. Shumeiko,*Charge transport in InAs nanowire Josephson junctions*, Phys. Rev. B 89, 214508 (2014).

[13] Y. Blum, A. Tsukernik, M. Karpovski, and A. Palevski ,*Critical current in Nb-Cu-Nb junctions with nonideal interfaces*, Phys. Rev. B 70, 214501 (2004).

[14] Previous work on graphene based SNS junctions mostly focused on the short junction regime [15–22]. The long junction diffusive regime was less but also investigated with graphene connected to Pb and Nb electrodes [23, 24] and very recently[25, 26] long ballistic junctions with MoW and Nb electrodes with very high transparency were investigated.

[15] H. B. Heersche, P. Jarillo-Herrero, J. B. Oostinga, L. M. K. Vandersypen, and A. F. Morpurgo,*Bipolar supercurrent in graphene*, Nature 446, 56 (2007).

[16] X. Du, I. Skachko, and E. Y. Andrei,*Josephson current and multiple Andreev reflections in graphene SNS junctions*, Phys. Rev. B 77, 184507 (2008).

[17] C. Girit et al.*Tunable graphene dc superconducting quantum interference device*, Nano Lett. 9, 1980 (2009).

[18] C. Ojeda-Aristizabal, M. Ferrier, S. Guéron, and H. Bouchiat,*Tuning the proximity effect in a superconductor-graphene-superconductor junction*, Phys. Rev. B 79, 165436 (2009).

[19] I. V. Borzenets, U. C. Coskun, S. J. Jones, and G. Finkel- stein,*Phase Diffusion in Graphene-Based Josephson Junctions* Phys. Rev. Lett. 107, 137005 (2011).

[20] F. Miao, W. Bao, H. Zhang and C.N. Lau, *Premature switching in graphene Josephson transistors*,Solid State Commun.149 , 1046 (2009).

[21] U. C. Coskun, M. Brenner, T. Hymel, V. Vakaryuk, A. Levchenko, A. Bezryadin. *Distribution of supercurrent switching in graphene under proximity effect.* Phys. Rev. Lett. 108, 097003 (2012).

[22] N. Mizuno, B. Nielsen, X. Du. *Ballistic-like supercurrent in suspended graphene Josephson weak links.* Nature Commun. 4, 3716 (2013).

[23] G.H. Lee, D. Jeong, Jae-Hyun Choi, Yong-Joo Doh, and Hu-Jong Lee, *Electrically Tunable Macroscopic Quantum Tunneling in a Graphene-Based Josephson Junction*, Phys. Rev. Lett. 107, 146605 (2011); Dongchan Jeong, Jae-Hyun Choi, Gil-Ho Lee, Sanghyun Jo, Yong-Joo Doh, and Hu-Jong Lee, *Observation of Supercurrent in PbIn-Graphene-PbIn Josephson Junction* Phys. Rev. B 83, 094503 (2011).

[24] Katsuyoshi Komatsu, Chuan Li, S. Autier-Laurent, H. Bouchiat, and S. Guéron *Superconducting proximity effect in long superconductor/graphene/superconductor junctions: From specular Andreev reflection at zero field to the quantum Hall regime* Phys. Rev. B 88, 115412 (2012).

[25] Victor E. Calado, Srijit Goswami, Gaurav Nanda, Mathias Diez, Anton R. Akhmerov, Kenji Watanabe, Takashi Taniguchi, Teun M. Klapwijk, Lieven M. K. Vandersypen *Ballistic Josephson junctions in edge-contacted graphene.*, Nat. Nano. 10, 761 (2015).

[26] M. Ben Shalom, M. J. Zhu, V. I. Fal'ko, A. Mishchenko, A. V. Kretinin, K. S. Novoselov, C. R. Woods, K. Watanabe, T. Taniguchi, A. K. Geim, J. R. Prance *Proximity superconductivity in ballistic graphene, from Fabry-Perot oscillations to random Andreev states in magnetic field*, Nature Physics (2015) (advanced online publication).

[27] The carrier density induced by the gate voltage is given by: $n_c = \frac{\varepsilon_r \varepsilon_0}{ed}|V_G - V_D|$, where $\varepsilon_r = 3.7$ for SiO_2, $\varepsilon_0 = 8.85 \times 10^{-12} F \cdot m^{-1}$, and $d = 285 \ nm$ is the thickness of the oxide layer. k_F is deduced from n_c via $k_F = \sqrt{\pi n_C} \simeq 4.75 \times 10^7 \times \sqrt{V_G - V_D} \ m^{-1}$.

[28] F Zhou, P Charlat, B Spivak, and B Pannetier. *Minigap in a long disordered SNS junction: Analytical results.* Physical Review B, **66**, 052507, (2002).

[29] A. Lodder, Yu. V. Nazarov *Density of states and the energy gap in Andreev billiards* PRB 58 5783 (1998).

[30] L. Angers, F. Chiodi, G. Montambaux, M. Ferrier, S. Guéron, H. Bouchiat, and J. Cuevas. *Proximity dc squids in the long-junction limit.* Physical Review B, 77, 165408, (2008).

[31] J. C. Hammer, J. C. Cuevas, F. S. Bergeret, W. Belzig,*Density of states and supercurrent in diffusive SNS junctions: Roles of nonideal interfaces and spin-flip scattering* Phys. Rev. B 76, 064514 (2007).

[32] Supplemental material.

[33] K. Flensberg, J. Bindslev Hansen, and M. Octavio, *Subharmonic energy-gap structure in superconducting weak links* Phys. Rev. B, 88, 8707 (1988).

[34] V. Ambegaokar and B.I. Halperin *Voltage Due to Thermal Noise in the dc Josephson Effect.*Phys. Rev. Lett. **22**, 1364,(1969).

[35] Supryo Datta "Electronic Transport in Mesoscopic Systems", Cambridge University Press (1995).

[36] F.K. Wilhelm, A.D. Zaikin, and G. Schön, *Supercurrent in a mesoscopic proximity wire*J. Low Temp. Phys. 106, 305 (1997).

[37] M. Ferrier, B. Dassonneville, S. Guéron, and H. Bouchiat *Phase-dependent Andreev spectrum in a diffusive SNS junction: Static and dynamic current response* Phys. Rev. B 88, 174505 (2013).

[38] We have chosen the superconducting gap $\Delta = t/4$ such that the S coherence length $\xi_s = at/\Delta \ll N_x^S$, to avoid suppressed superconducting correlations in the S (inverse proximity effect). The Fermi energy was chosen away from the Dirac point, at filling 1/4 . The disorder amplitude and l_e are related via $l_e = \alpha a(t/W)^2$ in 2D [39]. The number of transverse channels and disorder amplitude correspond to the diffusive regime, for which the normal region length $N_x a$ is greater than the elastic mean free path l_e and shorter than the localization length $N_y l_e$. T The coefficient α relating l_e to the amplitude of the disorder is determined from the 1/L dependence of the critical current in the short junction limit at $\tau = 1$.

[39] G. Montambaux, H. Bouchiat, D. Sigeti, and R. Friesner, *Persistent currents in mesoscopic metallic rings: Ensemble average*, Phys. Rev.B 42, 7647 (1990).